

The 9.7 Micron Silicate Dust Absorption Toward the Cygnus A Nucleus and the Inferred Location of the Obscuring Dust ¹

Masatoshi Imanishi ²

National Astronomical Observatory, Mitaka, Tokyo 181-8588, Japan

and

Shiro Ueno

Space Utilization Research Program, Tsukuba Space Center, National Space Development Agency of Japan, 2-1-1 Sengen, Tsukuba 305-8505, Japan

ABSTRACT

We report the detection of a 9.7 μm silicate dust absorption feature toward the Cygnus A nucleus. Its optical depth is, however, significantly smaller than that expected from the dust extinction toward the background L -band emission region ($A_V \sim 150$ mag). We argue that the most likely explanation for the small optical depth is that the obscuring dust exists so close to the central engine that a temperature gradient occurs. Our calculation confirms that the small optical depth and the spectral energy distribution at 3–30 μm can be quantitatively reproduced by this explanation. Combining this picture with the huge AGN luminosity, the emission properties of Cygnus A are consistent with those of a type 2 quasar, that is, a highly luminous AGN that is highly obscured ($A_V > 50$ mag) by a dusty torus with an inner radius of <10 pc, and not by $>$ a few 100 pc scale dust in the host galaxy.

Subject headings: galaxies: active — infrared: galaxies — galaxies: individual (Cygnus A) — galaxies: nuclei

¹ Data presented here were obtained at the W. M. Keck Observatory, which is operated as a scientific partnership among the California Institute of Technology, the University of California, and the National Aeronautics and Space Administration. The Observatory was made possible by the generous financial support of the W. M. Keck Foundation.

²Present address: Institute for Astronomy, University of Hawaii, 2680 Woodlawn Drive, Honolulu, Hawaii 96822, USA

1. Introduction

A wide range of the observed properties of active galactic nuclei (AGNs) can be explained by differing viewing angles toward a dusty torus with an inner radius of <10 pc around an accreting supermassive blackhole (Antonucci 1993). However, an important question about AGNs that has not yet been answered is “how common are type 2 quasars?” where we define type 2 quasars as highly luminous AGNs (bolometric luminosity of $>10^{12}L_{\odot}$, or 2–10 keV hard X-ray luminosity of $>10^{44}$ ergs s^{-1})³ that are highly obscured ($A_V > 50$ mag) by a dusty torus. To explain a significant fraction of the huge infrared luminosity of ultra-luminous infrared galaxies ($L_{\text{IR}} > 10^{12}L_{\odot}$; Sanders & Mirabel 1996) by dust emission powered by obscured AGN activity, the presence of such type 2 quasars is required. However, it has been suggested that dust around a highly luminous AGN is quickly expelled by strong radiation pressure and outflow activities, and therefore virtually no type 2 quasars exist (Halpern, Turner, & George 1999).

One way to search for a type 2 quasar is to find an X-ray source with a large hard X-ray to soft X-ray flux ratio (i.e., an indication of soft X-ray attenuation by absorption), and then perform optical follow-up spectroscopy to derive the redshift, and hence estimate the intrinsic hard X-ray luminosity (e.g., Sakano et al. 1998). If both the intrinsic 2–10 keV hard X-ray luminosity and X-ray absorption are estimated to be high (e.g., $L_X(2\text{--}10\text{ keV}) > 10^{44}$ ergs s^{-1} and $N_H > 10^{23}$ cm^{-2}), the source is a candidate type 2 quasar. However, X-ray absorption (N_H) is caused both by gas and dust, and the N_H/A_V ratio toward an AGN is often higher than that of the Galaxy ($N_H/A_V = 1.8 \times 10^{21}$ cm^{-2} mag $^{-1}$; Predehl & Schmitt 1995), as much as 10 times higher in some cases (Alonso-Herrero, Ward, & Kotilainen 1997; Simpson 1998). Hence, the estimation of dust obscuration (A_V) from hard X-ray absorption is highly uncertain. If the optical spectrum has sufficient spectral resolution and sensitivity, we can investigate dust obscuration by looking for the absence of a broad (> 2000 km s^{-1} in full width at half-maximum; FWHM) component of the rest-frame optical hydrogen emission lines (e.g., Ohta et al. 1996; Georgantopoulos et al. 1999). Its absence, however, indicates only that dust obscuration is at least several mag in A_V . Such a small amount of dust is insufficient to explain the huge amount of infrared emission by dust heated by AGN activity. Therefore, the question as to whether there are type 2 quasars that can explain the huge infrared luminosity by dust heated by obscured AGN activity cannot be answered explicitly by this method.

Study of thermal infrared regions (3–30 μm) is a powerful tool in the search for such a type 2 quasar. Firstly, since thermal infrared emission is visible through high

³ We adopt $H_0 = 75$ km s^{-1} Mpc $^{-1}$ and $q_0 = 0.5$ throughout this paper.

dust obscuration, as high as $A_V > 50$ mag, we can find a sample of highly luminous and highly dust obscured ($A_V > 50$ mag) AGNs. Secondly, we can examine the location of the obscuring dust. Obscuration can be either by dust in a dusty torus in the vicinity of a central engine (< 10 pc in inner radius), or by dust in the host galaxy ($>$ a few 100 pc scale). Needless to say, dust must be present in the location of the former in order for it to be heated by AGN activity. We can distinguish between these two possibilities by looking for the presence of a temperature gradient in the obscuring dust. If a dusty torus is responsible for the obscuration, a temperature gradient is predicted to occur, with the temperature of the dust decreasing with increasing distance from the central engine (Pier & Krolik 1992). The temperature of the innermost dust is expected to be ~ 1000 K, close to the dust sublimation temperature. Since emission at $3 \mu\text{m}$ is dominated by dust at ~ 1000 K, the extinction estimated using the $\sim 3 \mu\text{m}$ data should reflect the value toward the innermost dust around the central engine. On the other hand, the extinction estimated using $\sim 10 \mu\text{m}$ data should be lower, because the dust at ~ 300 K, a dominant emission source at $\sim 10 \mu\text{m}$, is located further out than the ~ 1000 K dust, and thus the $\sim 10 \mu\text{m}$ data can only trace the extinction toward the outer region. In fact, if there is a temperature gradient, the optical depth of the $9.7 \mu\text{m}$ silicate dust absorption is predicted to be lower than the actual column density toward the central engine (Pier & Krolik 1992). Such a temperature gradient is not thought to occur in the $>$ a few 100 pc scale dust in the host galaxy. Hence, comparing extinction estimates at $\sim 3 \mu\text{m}$ and $\sim 10 \mu\text{m}$ can provide useful information on the location of obscuring dust.

Cygnus A (3C 405; $z = 0.056$) has a highly luminous radio-loud AGN with a bolometric luminosity of $> 10^{45}$ ergs s^{-1} (Stockton, Ridgway, & Lilly 1994) and with an extinction-corrected 2–10 keV hard X-ray luminosity of $1\text{--}5 \times 10^{44}$ ergs s^{-1} (Ueno et al. 1994; Sambruna, Eracleous, & Mushotzky 1999). The dust extinction toward the background L -band ($\sim 3.5 \mu\text{m}$) emission region of the nucleus is estimated to be $A_V \sim 150$ mag, based on the comparison of the *observed* L -band luminosity to the predictions from the optical [OIII] emission line and the extinction-corrected 2–10 keV hard X-ray luminosities (Ward 1996). Both results suggest that Cygnus A is a candidate type 2 quasar, but a large scale central dust lane (e.g., Thompson 1984) rather than a dusty torus could be responsible for the high dust extinction. Although the 8–13 μm spectrum of Cygnus A has been presented by Ward (1996), neither the presence of the $9.7 \mu\text{m}$ silicate dust absorption feature nor its optical depth are clear due to limited signal-to-noise ratios. We conducted much more sensitive 8–13 μm spectroscopy to estimate the optical depth of the $9.7 \mu\text{m}$ silicate dust absorption feature, thereby to investigate the location of the obscuring dust.

2. Observation and Data Analysis

The 8–13 μm spectroscopy was conducted on the night of 1999, August 21 (UT) at the Keck I Telescope using the Long Wavelength Spectrometer (LWS; Jones & Puetter 1993) under photometric sky conditions. The seeing measured from a star was $\sim 0''.5$ in FWHM. The LWS used a 128×128 Si:As array. A low-resolution grating was used with a $0''.5$ wide slit and with an N-wide filter (8.1–13 μm). The resulting spectral resolution was ~ 50 .

We utilized a “chop and nod” technique (e.g., Miyata et al. 1999) to cancel the first order gradient of the sky emission variation and the difference in background signal between different chopping beams. The frame rate was 20 Hz. Following the measurements at Mauna Kea by Miyata et al. (1999), the chopping and nodding frequencies were set to 5 Hz and 1/30 Hz, respectively, to achieve a background-limited sensitivity. In the actual data, a background-limited sensitivity may not have been achieved, since stripe-like noise patterns were recognizable in the array. Since the emission region at 10 μm of Cygnus A and the standard star Vega ($=\alpha$ Lyrae, =HR7001) were spatially unresolved, $\sim 0''.5$ in FWHM, we set the chopping amplitude at $3''$ so as to maximize the observing efficiency by placing the objects on the array all the time in both the chopping and the nodding beams. The total on-source integration time of Cygnus A was 1650 sec. Vega was observed just before the Cygnus A observation, with an air mass difference less than 0.1, and was used as a spectroscopic standard star.

We followed a standard data analyzing procedure, using IRAF⁴. We first defined high dark current pixels and low-sensitivity pixels using, respectively, the dark and blackbody frames taken just after the Cygnus A observation. We replaced the data of these pixels with the interpolated signals of the surrounding pixels. The slit positions were nearly the same for Cygnus A and Vega, but the signal positions on the slit were slightly different. We corrected for the pixel variation of quantum efficiency along the slit by using the blackbody frame, whose flux was uniform along the slit. We extracted the spectra of the target and the standard star using an optimal extraction algorithm.

The wavelengths were calibrated using sky lines. The Earth’s atmospheric transmission shows small and narrow dips at 11.7 μm and 12.6 μm (Tokunaga 1998) that are easily discernible in raw images as local maxima of sky background emission. We examined the positions of these two local maxima and confirmed that the wavelength per pixel was 0.043 arcsec pixel⁻¹, consistent with the designed value. We therefore calibrated the wavelengths

⁴ IRAF is distributed by the National Optical Astronomy Observatories, which are operated by the Association of Universities for Research in Astronomy, Inc. (AURA), under cooperative agreement with the National Science Foundation.

by assuming a linear relationship between wavelength and pixel of $0.043 \text{ arcsec pixel}^{-1}$ throughout the detector. In the wavelength-calibrated data, a broad local maximum of sky background emission is found at $9.3\text{--}9.7 \mu\text{m}$. This wavelength range corresponds to the broad local minimum of the Earth’s atmospheric transmission (Tokunaga 1998). This wavelength calibration is believed to be accurate to within $0.05 \mu\text{m}$.

Although Vega is known to show an infrared excess at $>20 \mu\text{m}$, the excess is not appreciable at $<15 \mu\text{m}$ (Heinrichsen, Walker, & Klaas 1998). We divided the signals of Cygnus A by those of Vega and multiplied the result by a blackbody profile of 9400 K (Cohen et al. 1992). In our spectroscopy, because the slit width was comparable to the seeing, some signal was possibly lost due to slight tracking errors; thus a high ambiguity in flux calibration may be introduced. We calibrated the flux of Cygnus A in such a way that our spectrum between $8.1 \mu\text{m}$ and $13 \mu\text{m}$ agreed with the N -band photometric data ($N = 0.18 \text{ Jy}$ or 5.7 mag ; Rieke & Low 1972; Heckman et al. 1983). The flux measurement using our data agrees with this by a factor of ~ 2 .

3. Results

The flux-calibrated spectrum of Cygnus A is shown in Figure 1. A broad absorption-like feature is seen at a peak wavelength of $\sim 10 \mu\text{m}$. This wavelength is consistent to the peak wavelength of the $9.7 \mu\text{m}$ silicate dust absorption feature redshifted with $z = 0.056$. Hence, the broad absorption-like feature is likely to originate from silicate dust absorption.

It has been suggested that, if a galaxy is powered strongly by star-formation activities, and the polycyclic aromatic hydrocarbon (PAH) emission features at $7.7 \mu\text{m}$, $8.6 \mu\text{m}$, and $11.3 \mu\text{m}$ are strong, then the mid-infrared spectra mimic those with $9.7 \mu\text{m}$ silicate dust absorption (Genzel et al. 1998). In the case of Cygnus A, however, the extinction-corrected $2\text{--}10 \text{ keV}$ hard X-ray luminosity ($L_X(2\text{--}10 \text{ keV}) = 1\text{--}5 \times 10^{44} \text{ ergs s}^{-1}$) relative to the $40\text{--}500 \mu\text{m}$ far-infrared luminosity ($L_{\text{FIR}} = 0.7\text{--}1.6 \times 10^{45} \text{ ergs s}^{-1}$)⁵ is $\gtrsim 0.1$, as high as in galaxies powered predominantly by AGN activity. Furthermore, the wavelength coverage of our spectrum ($8.1\text{--}13.0 \mu\text{m}$) is $7.7\text{--}12.3 \mu\text{m}$ in the rest-frame and hence covers the $11.3 \mu\text{m}$ PAH emission feature ($10.9\text{--}11.6 \mu\text{m}$ in the rest-frame; Rigopoulou et al. 1999). We find no detectable $11.3 \mu\text{m}$ PAH emission feature at $11.9 \mu\text{m}$ in the observed frame ($<6 \times 10^{-17} \text{ W m}^{-2}$ in flux or $<4 \times 10^{41} \text{ ergs s}^{-1}$ in luminosity). The $11.3 \mu\text{m}$ PAH to far-infrared

⁵ We use the formula $L_{\text{FIR}} = 2.1 \times 10^{39} \times D(\text{Mpc})^2 \times (2.58 \times f_{60} + f_{100})$, where f_{60} and f_{100} are, respectively, the *IRAS* $60 \mu\text{m}$ and $100 \mu\text{m}$ flux in Jy (Sanders & Mirabel 1996). The f_{60} and f_{100} fluxes of Cygnus A are 2.329 Jy and $<8.278 \text{ Jy}$, respectively.

40–500 μm luminosity ratio is $<6 \times 10^{-4}$, more than an order of magnitude smaller than that found for galaxies powered by star-formation activities (0.009 ± 0.003 ; Smith, Aitken, & Roche 1989). Hence, it is very unlikely that the shorter side of our mid-infrared spectrum is dominated by PAH emission features from star-formation activities. We therefore ascribe the broad absorption-like feature fully to 9.7 μm silicate dust absorption.

4. Discussion

4.1. The Small Optical Depth of Silicate Dust Absorption

Since the Galactic dust extinction toward the Cygnus A nucleus is estimated to be small, $A_V \sim 1$ mag (Spinrad & Stauffer 1982; van den Bergh 1976), the 9.7 μm silicate dust absorption is believed to be attributed to dust in the Cygnus A galaxy. If we adopt the ratio of visual extinction to the optical depth of the 9.7 μm silicate dust absorption found in the Galactic interstellar medium ($A_V/\tau_{9.7} = 9\text{--}19$; Roche & Aitken 1985), a dust extinction of $A_V \sim 150$ mag should provide $\tau_{9.7} = 7.9\text{--}16.6$. In this case, the flux at the absorption peak should be attenuated by a factor of $2.7 \times 10^3 - 1.6 \times 10^7$, and hence should be saturated in the spectrum. The observed spectrum, however, shows no such saturation at all. If we use the following formula by Aitken & Jones (1973),

$$\tau_{9.7} = \ln \left[\frac{F_\lambda(8) + F_\lambda(13)}{2 \times F_\lambda(9.7)} \right] \text{ (rest-frame),}$$

then $\tau_{9.7}$ is only ~ 1 , much smaller than that expected from $A_V \sim 150$ mag. This is the predicted trend when obscuring dust exists so close to a central engine that a temperature gradient occurs. Before pursuing this possibility in more detail, we review another possibility that could explain the small $\tau_{9.7}$.

Interstellar dust consists mainly of silicate and carbonaceous dust (Mathis, Rumpl, & Nordsieck 1977; Mathis & Whiffen 1989). If the contribution of silicate dust to A_V is much smaller than that in the Galactic interstellar medium, $\tau_{9.7}$ could be small even in the case of high A_V . However, since carbonaceous dust is more fragile than silicate dust (Draine & Salpeter 1979), carbonaceous dust should have been more destroyed than silicate dust around the Cygnus A nucleus, where a radiation field is expected to be much stronger and more energetic than that in the Galactic interstellar medium. The depletion of silicate dust relative to carbonaceous dust around Cygnus A is very unlikely. We therefore argue that a temperature gradient is the most likely explanation that could reproduce the observed small $\tau_{9.7}$.

4.2. Modeling

In this subsection, we examine whether a temperature gradient can *quantitatively* explain the small $\tau_{9.7}$ in spite of a high A_V toward the background L -band emission region. In addition to our mid-infrared spectrum, we incorporate data points at 3–30 μm to constrain our model parameters. This is because dust emission powered by obscured AGN activity is strong at 3–30 μm and thus emission in this wavelength range can provide useful information on the dust distribution around a central engine. The photometric data at 3–30 μm used are summarized in Table 1. We do not incorporate data at $<3 \mu\text{m}$ and at $>30 \mu\text{m}$, because stellar emission dominates the flux of Cygnus A at $<3 \mu\text{m}$ (Djorgovski et al. 1991), while emission from cold dust in the host galaxy could contribute significantly at $>30 \mu\text{m}$.

We estimate the contribution of (1) synchrotron emission and (2) stellar emission to the 3–30 μm emission of Cygnus A. Firstly, the spectral energy distribution of the Cygnus A nucleus (without hotspots emission) shows a clear flux excess in the infrared regions compared to the extrapolation of the synchrotron emission component at longer wavelengths (Haas et al. 1998). In fact, if we extrapolate the data at 0.45–2.0 mm using $F_\nu \propto \nu^{-0.6}$ (Robson et al. 1998) and assume an extinction of $A_V = 150$ mag toward the synchrotron emission region of the Cygnus A nucleus, then we find the synchrotron emission component contributes less than 1/10 of the observed flux at 3–30 μm . Secondly, the contribution from the stellar emission can be estimated from the near-infrared K -band (2.2 μm) photometric data ($K = 13.78 \pm 0.06$ mag), which are dominated by stellar emission in the case of Cygnus A (Djorgovski et al. 1991). If we assume the $K - L$ and $K - L'$ colors of late type stellar populations in normal galaxies (0.2–0.4; Willner et al. 1984), the stellar contribution at L and L' is 13.4–13.6 mag. This is smaller than $\sim 30\%$ of the observed flux at L and L' . At wavelengths longer than L' , the stellar contribution decreases and becomes negligible.

As a consequence, the 3–30 μm data of Cygnus A should be dominated by dust emission powered by obscured AGN activity. We use the code *DUSTY* developed by Ivezić, Nenkova, & Elitzur (1999) to investigate whether the observed small $\tau_{9.7}$ as well as the spectral energy distribution at 3–30 μm can be quantitatively explained by emission from dust in the vicinity of a central AGN.

The code *DUSTY* solves the radiative transfer equation for a source embedded in a spherically symmetric dusty envelope. It creates an output spectrum as the sum of the attenuated input radiation, dust emission, and scattered radiation. For Cygnus A, the presence of radio hot spots (Wright & Birkinshaw 1984), the detection of strong optical [OIII] emission (Osterbrock & Miller 1975), and centrosymmetric polarization patterns (Tadhunter, Scarrott, & Rolph 1990; Ogle et al. 1997) indicate that the dusty envelope is torus-like, with dust along an unknown direction roughly perpendicular to our line of

sight expelled with an unknown solid angle. Hence, strictly speaking, the assumption of spherical symmetry is not valid. If we view the torus-like structure from a face-on direction where the unattenuated hot (~ 1000 K) dust emission from the innermost envelope is seen directly, the output dust emission spectrum is expected to be quite different to the one from a spherical dusty envelope around a central engine, because all the hot dust emission is attenuated in the spherical model. However, it is most likely in the case of Cygnus A that we are viewing the torus from almost an edge-on direction, where no unattenuated emission from the innermost envelope is seen. Furthermore, because our aim is to explain the small $\tau_{9.7}$, the presence of a temperature gradient in the obscuring dust along our line of sight in front of a background emitting source is the most important factor. The geometry of dust perpendicular to our line of sight would not be crucial. Hence, for simplicity, we assume a spherically symmetric dust envelope.

Thanks to the general scaling properties of the radiative transfer mechanism (Rowan-Robinson 1980; Ivezić & Elitzur 1997), there are only several free parameters. Firstly, we assume the input radiation as blackbody with a temperature of 40000 K, following Rowan-Robinson & Efstathiou (1993). This is not very critical as explained by Rowan-Robinson (1980). Next, we set the dust sublimation temperature as 1000 K following Rowan-Robinson & Efstathiou (1993) and Dudley & Wynn-Williams (1997). Since, in this model, the extinction estimated using $\sim 3 \mu\text{m}$ data is believed to be nearly the same as the extinction toward the central engine (§ 1), we set the optical depth at $0.55 \mu\text{m}$ ($\sim A_V/1.08$) toward the central engine to $\tau = 140$. We adopt the standard dust size distribution by Mathis et al. (1977) and standard interstellar dust mixture as defined in *DUSTY*. The ratio of the outer to the inner radius of the dusty envelope is set as a free parameter. We only try a simple power law radial density profile ($\propto r^\gamma$), and the value γ is also set as a free parameter.

When searching for parameters that can fit the observed data, we allow the model output spectrum and the observed data to differ by a few factors, particularly at shorter wavelengths. This is because the period over which the data in Table 1 were taken spans 10 years. Since emission at shorter wavelengths is from warm dust located at the inner part of a dusty envelope, variability over a time scale of 10 years could be significant.

In Figure 2, we show the results of a calculation that provides a reasonable fit to the observed data, particularly at longer wavelengths. The outer-to-inner radius ratio is 200, and the power-law index of dust radial distribution is 2.5. If we adopt a value of $\sim 10^{45}$ ergs s^{-1} as the luminosity of the central radiation source, the physical scales of the inner radius of the dusty envelope is 2.25 pc. An outer-to-inner radius ratio of 80–500 and a power-law index of 2.5–3.0 for the dust radial distribution produce an output spectrum similar to that

shown in Figure 2.

In summary, the observed small $\tau_{9.7}$ as well as the spectral energy distribution at 3–30 μm of Cygnus A can be quantitatively explained by a model in which the emission at 3–30 μm originates from thermal emission by dust in the vicinity of a central AGN. Combining this result with the huge AGN luminosity of Cygnus A ($L_X(2\text{--}10\text{ keV}) > 10^{44}\text{ ergs s}^{-1}$), we argue that observed data are consistent with the picture of Cygnus A being a type 2 quasar, that is, a highly luminous AGN that is highly obscured ($A_V > 50\text{ mag}$) not by $>$ a few 100 pc scale dust in the host galaxy, but by a dusty torus with an inner radius of $<10\text{ pc}$.

4.3. Another type 2 quasar

Although we demonstrated that the observed data are consistent with the picture of Cygnus A being a type 2 quasar, Cygnus A is a radio-loud AGN (the minor AGN population) and is a cD galaxy at the center of a cluster of galaxies (Spinrad & Stauffer 1982). It may be thought that Cygnus A is an unusual example. In this subsection, we mention briefly the emission properties of a radio-*quiet* AGN (the major AGN population), IRAS 08572+3915.

IRAS 08572+3915 ($z = 0.058$) is one of the nearby ultra-luminous infrared galaxies ($L_{\text{IR}} > 10^{12} L_{\odot}$; Kim, Veilleux, & Sanders 1998). The radio 20 cm to the far-infrared 40–500 μm flux ratio is similar to those of radio-quiet AGNs (Crawford et al. 1996). It displays a strong absorption-like feature at 10 μm (Dudley & Wynn-Williams 1997). Although the interpretation of the absorption-like feature at $\sim 10\text{ }\mu\text{m}$ is sometimes difficult (§ 3), this source displays a very strong 3.4 μm carbonaceous dust absorption feature and no detectable 3.3 μm PAH emission feature in the 3–4 μm spectrum (Wright et al. 1996), strongly suggesting that IRAS 08572+3915 is powered by a highly embedded AGN and not by star-formation activities⁶. Hence, the strong absorption-like feature at $\sim 10\text{ }\mu\text{m}$ must be fully attributed to 9.7 μm silicate dust absorption. Based on the optical depth ratio between the 9.7 μm and 18 μm silicate dust absorption features, the presence of a temperature gradient in the obscuring dust around a very compact energy source (= AGN) has been argued (Dudley & Wynn-Williams 1997). If we adopt $\tau_{9.7} = 5.2$ (Dudley & Wynn-Williams

⁶Dudley & Wynn-Williams (1997) argue that the 8–22 μm spectrum of Arp 220 and that of IRAS 08572+3915 share similar properties. However, another interpretation of the 10 μm spectrum of Arp 220 has been proposed by Genzel et al. (1998). Given the absence of a high-quality 3–4 μm spectrum of Arp 220, it is unknown which interpretation is correct. In this paper we tentatively regard only IRAS 08572+3915 as a convincing sample of a type 2 quasar.

1997) and the Galactic optical depth ratio of the $3.4 \mu\text{m}$ carbonaceous to the $9.7 \mu\text{m}$ silicate dust absorption ($\tau_{3.4}/\tau_{9.7} = 0.06\text{--}0.07$; Pendleton et al. 1994; Roche & Aitken 1985), then $\tau_{3.4} \sim 0.35$ is expected. The observed $\tau_{3.4}$ is ~ 0.9 (Pendleton 1996), more than a factor of 2 higher than expected. This means the extinction estimate at $\sim 3 \mu\text{m}$ is higher than that at $\sim 10 \mu\text{m}$ and thus supports the presence of a temperature gradient in the obscuring dust around the AGN. All the results are consistent with the picture of IRAS 08572+3915 being a radio-quiet type 2 quasar.

IRAS 08572+3915 has a LINER-type optical spectrum (Kim et al. 1998). No broad ($> 2000 \text{ km s}^{-1}$ in FWHM) emission line has been detected in the $2 \mu\text{m}$ spectrum (Veilleux, Sanders, & Kim 1999). The detection of 2–10 keV hard X-ray flux by the Advanced Satellite for Cosmology and Astrophysics (*ASCA*) is at most marginal (based on our quick look into the *ASCA* archive). Namely, no sign of strong AGN activity has been detected at $< 2 \mu\text{m}$ or even at hard X-ray. The weak hard X-ray flux is not surprising, given the high obscuration toward the nucleus. The estimated A_V toward the $3 \mu\text{m}$ emission region (that is, toward the innermost part of the obscuring dust) from the observed $\tau_{3.4}$ is 130–220 mag, if we adopt the relation $\tau_{3.4}/A_V = 0.004\text{--}0.007$ found in the Galactic interstellar medium (Pendleton et al. 1994). If the dust-to-gas ratio is more than a factor of five higher than the Galactic value ($N_{\text{H}}/A_V = 1.8 \times 10^{21} \text{ cm}^{-2} \text{ mag}^{-1}$), as observed in some AGNs (see § 1), then N_{H} is higher than 10^{24} cm^{-2} , and direct 2–10 keV hard X-ray emission is completely blocked.

Unlike Cygnus A, the signs of a type 2 quasar in IRAS 08572+3915 were first recognized through study of thermal infrared regions. We suggest that other type 2 quasars that are not recognizable at $< 2 \mu\text{m}$ and at hard X-ray region may also be found through detailed study of the thermal infrared region.

5. Summary

Our main results are the following.

1. We detected a $9.7 \mu\text{m}$ silicate dust absorption feature toward the Cygnus A nucleus.
2. The optical depth of the absorption feature ($\tau_{9.7} \sim 1$) is smaller by a large factor than that expected from A_V toward the background *L*-band emission region (~ 150 mag).
3. We demonstrated that the small optical depth together with the spectral energy distribution at 3–30 μm could be quantitatively explained by emission from a dusty envelope in the vicinity ($< 10 \text{ pc}$ in inner radius) of a central AGN.

4. Combining this finding with the huge AGN luminosity of Cygnus A, we argued that the observed data are consistent with the picture of Cygnus A being a type 2 quasar.

We thank R. Campbell and T. Stickel for their support during the Keck observing run, Dr. C. C. Dudley for his useful comments on the manuscript, and L. Good for her proofreading of this paper. Drs. A. T. Tokunaga and H. Ando support my stay at the University of Hawaii. MI is financially supported by the Japan Society for the Promotion of Science during his stay at the University of Hawaii.

REFERENCES

- Aitken, D. K., & Jones, B., 1973, *ApJ*, 184, 127
- Alonso-Herrero, A., Ward, M. J., & Kotilainen, J. K. 1997, *MNRAS*, 288, 977
- Antonucci, R. 1993, *ARA&A*, 31, 473
- Cohen, M., Walker, R. G., Barlow, M. J., & Deacon, J. R. 1992, *AJ*, 104, 1650
- Crawford, T., Marr, J., Partridge, B., & Strauss, M. A. 1996, *ApJ*, 460, 225
- Djorgovski, S., Weir, N., Matthews, K., & Graham, J. R. 1991, *ApJ*, 372, L67
- Draine, B. T., & Salpeter, E. E. 1979, *ApJ*, 231, 438
- Dudley, C. C., & Wynn-Williams, C. G. 1997, *ApJ*, 488, 720
- Genzel, R. et al. 1998, *ApJ*, 498, 579
- Georgantopoulos, I., Almaini, O., Shanks, T., Stewart, G. C., Griffiths, R. E., Boyle, B. J., & Gunn, K. F. 1999, *MNRAS*, 305, 125
- Haas, M., Chini, R., Meisenheimer, K., Stickel, M., Lemke, D., Klaas, U., & Kreysa, E. 1998, *ApJ*, 503, L109
- Halpern, J. P., Turner, T. J., & George, I. M. 1999, *MNRAS*, 307, L47
- Heckman, T. M., Lebofsky, M. J., Rieke, G. H., & Van Breugel, W. 1983, *ApJ*, 272, 400
- Heinrichsen, I., Walker, H. J., & Klaas, U. 1998, *MNRAS*, 293, L78
- Ivezic, Z., & Elitzur, M. 1997, *MNRAS*, 287, 799
- Ivezic, Z., Nenkova, M., & Elitzur, M. 1999, *astro-ph/9910475*
- Jones, B., & Puetter, R. C. 1993, *Proc. SPIE*, 1946, 610
- Kim, D. -C., Veilleux, S., & Sanders, D. B. 1998, *ApJ*, 508, 627
- Mathis, J. S., & Whiffen, G. 1989, *ApJ*, 341, 808
- Mathis, J. S., Rumpl, W., Nordsieck, K. H. 1977, *ApJ*, 217, 425
- Miyata, T., Kataza, H., Okamoto, Y., Tanabe, T., Onaka, T., Yamashita, T., Nakamura, K., & Shibai, H. 1999, *PASP*, 111, 750

- Ogle, P. M., Cohen, M. H., Miller, J. S., Tran, H. D., Fosbury, R. A. E., & Goodrich, R. W. 1997, *ApJ*, 482, L37
- Ohta, K., Yamada, T., Nakanishi, K., Ogasaka, Y., Kii, T., & Hayashida, K. 1996, *ApJ*, 458, L57
- Osterbrock, D. E., & Miller, J. S. 1975, *ApJ*, 197, 535
- Pendleton, Y. 1996, in *The Cosmic Dust Connection*, Greenberg, J. M., ed., Kluwer Academic Publishers, p.71
- Pendleton, Y. J., Sandford, S. A., Allamandola, L. J., Tielens, A. G. G. M., & Sellgren, K. 1994, *ApJ*, 437, 683
- Pier, E. A., & Krolik, J. H. 1992, *ApJ*, 401, 99
- Predehl, P., & Schmitt, J. H. M. M. 1995, *A&A*, 293, 889
- Rieke, G. H., & Low, F. J. 1972, *ApJ*, 176, L95
- Rigopoulou, D., Spoon, H. W. W., Genzel, R., Lutz, D., Moorwood, A. F. M., & Tran, Q. D. 1999, *astro-ph/9908300*
- Robson, E. I., Leeuw, L. L., Stevens, J. A., & Holland, W. S. 1998, *MNRAS*, 301, 935
- Roche, P. F., & Aitken, D. K. 1985, *MNRAS*, 215, 425
- Rowan-Robinson, M. 1980, *ApJS*, 44, 403
- Rowan-Robinson, M., & Efstathiou, A. 1993, *MNRAS*, 263, 675
- Sakano, M., et al. 1998, *ApJ*, 505, 129S
- Sambruna, R. M., Eracleous, M., & Mushotzky, F. 1999, *ApJ*, 526, 60
- Sanders, D. B., & Mirabel, I. F. 1996, *ARA&A*, 34, 749
- Simpson, C. 1998, *ApJ*, 509, 653
- Smith, C.H., Aitken, D. K., & Roche, P. F. 1989, *MNRAS*, 241, 425
- Spinrad, H., & Stauffer, J. R. 1982, *MNRAS*, 200, 153
- Stockton, A., Ridgway, S. E., & Lilly, S. J. 1994, *AJ*, 108, 414
- Tadhunter, C. N., Scarrott, S. M., & Rolph, C. D. 1990, *MNRAS*, 246, 163

- Thompson, L. A., 1984, ApJ, 279, L47
- Tokunaga, A. T. 1998, Astrophysical Quantities, 4th Edition, Cox, A., ed, Springer-Verlag, Chapter 7
- Ueno, S., Koyama, K., Nishida, M., Yamauchi, S., & Ward, M. L. 1994, ApJ, 431, L1
- van den Bergh, S., 1976, ApJ, 210, L63
- Veilleux, S., Sanders, D. B., & Kim, D. -C. 1999, ApJ, 522, 139
- Ward, M. J. 1996, in Cygnus A - Study of a Radio Galaxy, Carilli, C. L., & Harris, D. E., eds, Cambridge University Press, p.43
- Willner, S. P., Ward, M., Longmore, A., Lawrence, A., Fabbiano, G., & Elvis, M., 1984, ApJ, 96, 143
- Wright, G. S., Bridger, A., Geballe, T. R., & Pendleton, Y. 1996, New Extragalactic Perspectives in the New South Africa, Kluwer Academic Publishers, Block, D. L., & Greenberg, J. M., (eds), p.143
- Wright, M., & Birkinshaw, M. 1984, ApJ, 281, 135

Table 1. Photometric Data of Cygnus A at 3–30 μm

Wavelength (μm)	Flux (Jy)	Reference
3.55 (<i>L</i>)	$(8.5 \pm 1.0) \times 10^{-3}$ ($11.28_{-0.12}^{+0.14}$ mag)	Heckman et al. (1983)
3.75 (<i>L'</i>)	$(3.8_{-1.2}^{+1.6}) \times 10^{-3}$ (12.05 ± 0.4 mag)	Djorgovski et al. (1991)
4.8	<0.030	Haas et al. (1998)
7.3	0.061	Haas et al. (1998)
12	<0.250	<i>IRAS</i> Point Source Catalog
12.8	0.485	Haas et al. (1998)
20	0.816	Haas et al. (1998)
25	1.062	<i>IRAS</i> Point Source Catalog

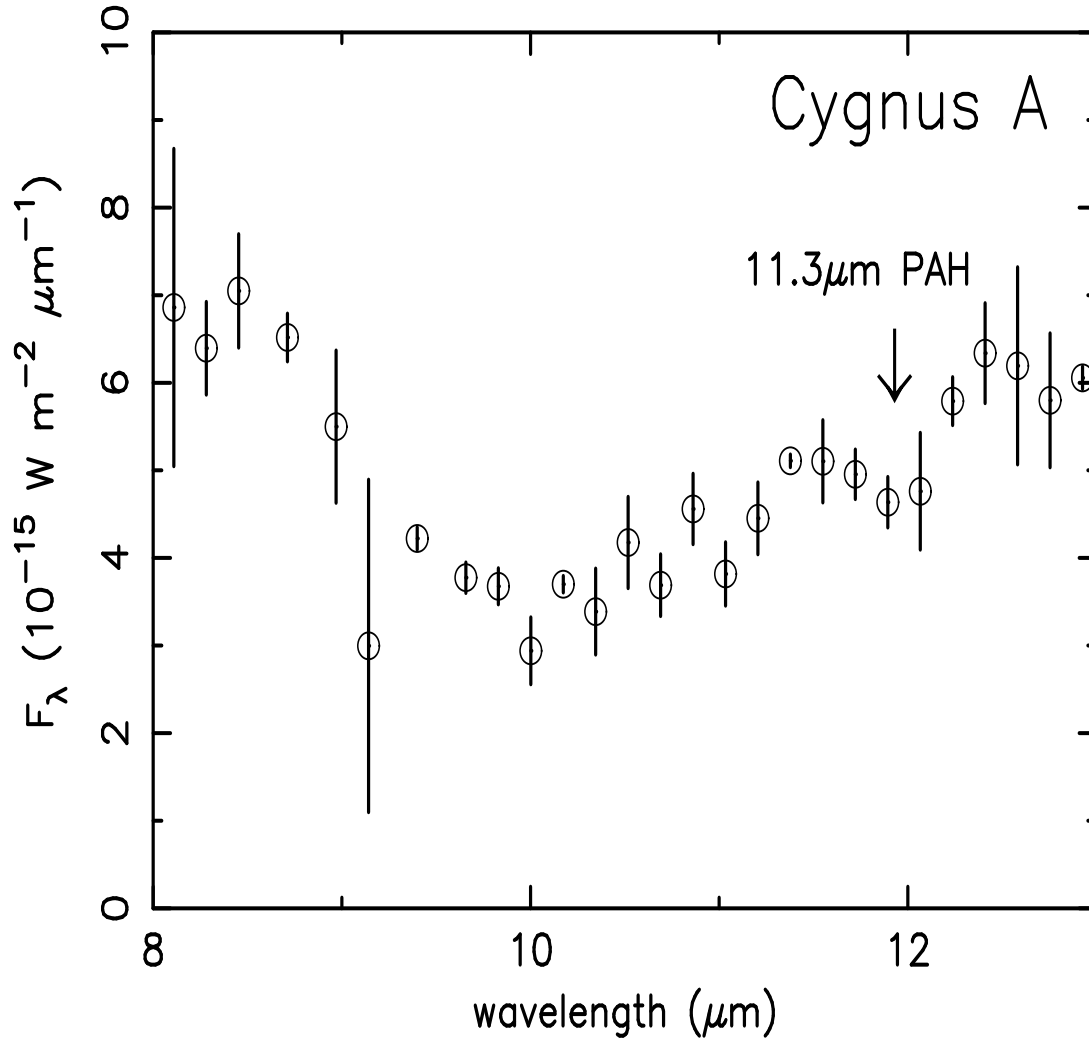


Fig. 1.— Flux-calibrated spectrum of Cygnus A. The ordinate is F_λ in $\text{W m}^{-2} \mu\text{m}^{-1}$, and the abscissa is wavelength in μm in the observed frame. The down arrow indicates the wavelength of the redshifted 11.3 μm PAH emission feature.

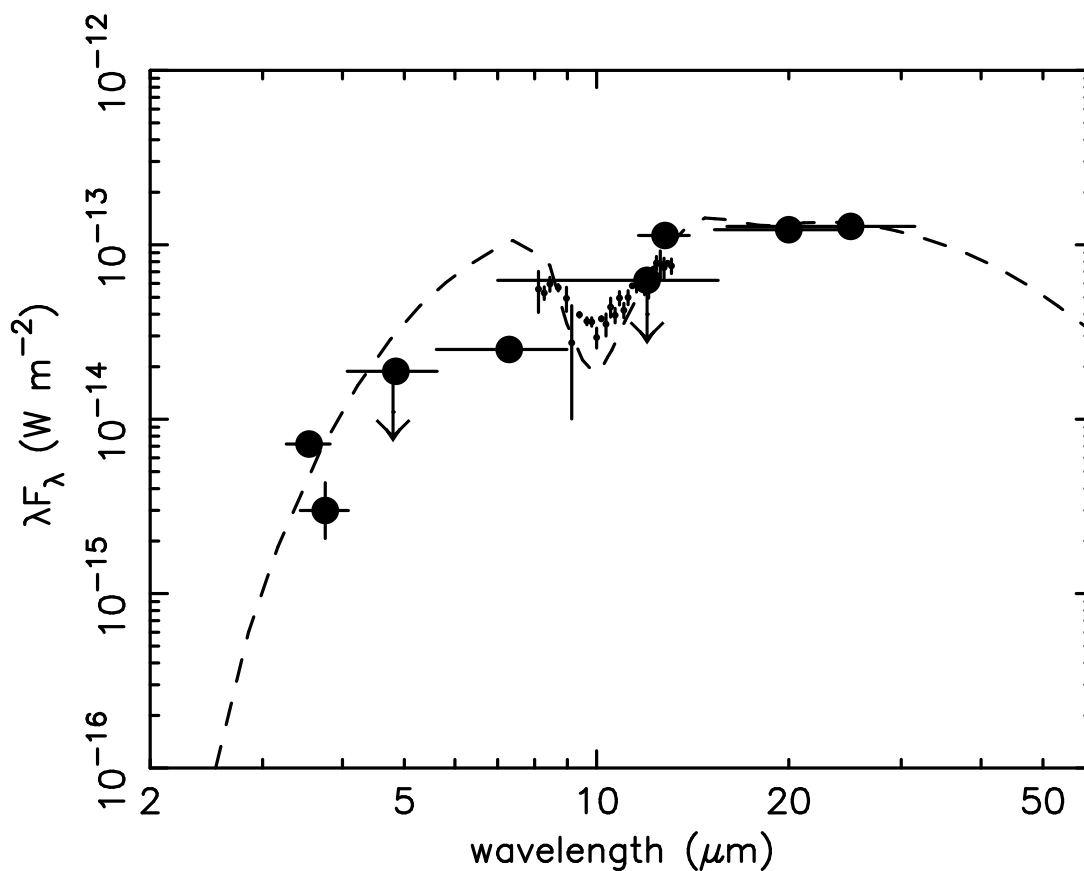


Fig. 2.— Spectral energy distribution of Cygnus A at 3–30 μm . The ordinate is λF_λ in W m^{-2} , and the abscissa is wavelength in μm in the observed frame. The dashed line is the output spectrum of *DUSTY* with an outer-to-inner radius ratio of 200, a power-law index of 2.5 in the dust radial distribution, and an optical depth at 0.55 μm of 140 toward the central engine. Large filled circles: Data from the literature (Table 1). Small filled circles: Our LWS data. Any model output spectra that fit the observed data at $>10 \mu\text{m}$ overpredict the fluxes at 4.8 and 7.3 μm . This could be caused by time variation (see § 4.2).